



# Foxo3 circular RNA promotes cardiac senescence by modulating multiple factors associated with stress and senescence responses

William W. Du<sup>1,2</sup>, Weining Yang<sup>1</sup>, Yu Chen<sup>3</sup>, Zhong-Kai Wu<sup>3</sup>, Francis Stuart Foster<sup>1</sup>, Zhenguo Yang<sup>1,2</sup>, Xiangmin Li<sup>1,2,4</sup>, and Burton B. Yang<sup>1,2,5\*</sup>

<sup>1</sup>Sunnybrook Research Institute, Sunnybrook Health Sciences Centre, Toronto, Canada; <sup>2</sup>Department of Laboratory Medicine and Pathobiology, University of Toronto, S-Wing Research Building, 2075 Bayview Ave, Toronto M4N 3M5, Canada; <sup>3</sup>2nd Department of Cardiac Surgery, The First Hospital, Sun Yet-Sen University, Guangzhou, China; <sup>4</sup>State Key Laboratory of Applied Microbiology Southern China (The Ministry-Province Joint Development), Guangdong Institute of Microbiology, Guangzhou 510070, PR China; and <sup>5</sup>Institute of Medical Science, University of Toronto, Toronto, Canada

Received 14 May 2015; revised 22 December 2015; accepted 31 December 2015

## Aims

Circular RNAs are a subclass of non-coding RNAs detected within mammalian cells. This study was designed to test the roles of a circular RNA circ-Foxo3 in senescence using *in vitro* and *in vivo* approaches.

## Methods and results

Using the approaches of molecular and cellular biology, we show that a circular RNA generated from a member of the forkhead family of transcription factors, Foxo3, namely circ-Foxo3, was highly expressed in heart samples of aged patients and mice, which was correlated with markers of cellular senescence. Doxorubicin-induced cardiomyopathy was aggravated by ectopic expression of circ-Foxo3 but was relieved by silencing endogenous circ-Foxo3. We also found that silencing circ-Foxo3 inhibited senescence of mouse embryonic fibroblasts and that ectopic expression of circ-Foxo3 induced senescence. We found that circ-Foxo3 was mainly distributed in the cytoplasm, where it interacted with the anti-senescent protein ID-1 and the transcription factor E2F1, as well as the anti-stress proteins FAK and HIF1 $\alpha$ .

## Conclusion

We conclude that ID-1, E2F1, FAK, and HIF1 $\alpha$  interact with circ-Foxo3 and are retained in the cytoplasm and could no longer exert their anti-senescent and anti-stress roles, resulting in increased cellular senescence.

## Keywords

Circular RNA • Heart senescence • Foxo3 • Stress response

## Translational perspective

The circular RNA circ-Foxo3 is highly expressed in hearts of aged mice and patients and correlated with extensive senescence. Ectopic expression of circ-Foxo3 induced senescence and aggravated doxorubicin-induced cardiomyopathy. Silencing endogenous circ-Foxo3 inhibited senescence and relieved cardiomyopathy. This occurred through interaction with anti-senescent proteins ID-1 and E2F1, as well as anti-stress proteins FAK and HIF1 $\alpha$ , leading to the relocation of these proteins in cytoplasm. Circ-Foxo3 may be targeted for drug development in the inhibition of tissue senescence.

## Introduction

Senescence is the gradual deterioration of bodily function and the leading cause of death, which can occur at either the cellular level or at the organismal level.<sup>1</sup> Cellular senescence, also known as replicative senescence, is characterized by halted mitosis of diploid

cells, while organismal senescence is characterized by a reduced stress response and increased homeostatic imbalance, resulting in a loss of normal functions to the organisms.<sup>2</sup> Cellular senescence is the cellular basis of organismal aging and is a useful model for studying organismal aging.<sup>3</sup> Cellular senescence is defined as the arrest of cell cycle progression,<sup>4</sup> which can be caused by telomere

\* Corresponding author. Tel: +1 416 480 5874, Fax: 1 416 480 5737, Email: [byang@sri.utoronto.ca](mailto:byang@sri.utoronto.ca)

Published on behalf of the European Society of Cardiology. All rights reserved. © The Author 2016. For permissions please email: [journals.permissions@oup.com](mailto:journals.permissions@oup.com).

shortening or stress-induced premature senescence.<sup>5</sup> This is characterized by a flattened and enlarged cell morphology, and lysosomal activation, resulting in positive staining of senescence-associated  $\beta$ -galactosidase activity (SA- $\beta$ -gal).<sup>6</sup> Stress can induce premature senescence and activate many markers similar to those in replicative senescence. Various experimental stressors, including oxidative stressor such as hydrogen peroxide, have been used to model cellular senescence within a short period of time.<sup>3</sup> Using this model system, we have recently demonstrated that cardiac fibroblast senescence is regulated by miR-17, which targets the senescent protein Par4.<sup>7</sup> We also found that the inhibition of senescence by miR-17 resulted in retardation of tissue growth<sup>8</sup> and extension of mouse lifespan<sup>9</sup> by regulating a number of senescence and stress-associated proteins. In organismal stress, a chemotherapeutic drug Doxorubicin (Dox) is extensively used to generate reactive oxidative stress and to induce cell apoptosis, leading to myocardial dysfunction.<sup>10</sup>

This study was designed to test the roles of a circular RNA (circRNA) circ-Foxo3 in senescence using *in vitro* and *in vivo* approaches. CircRNAs are a large group of non-coding RNAs that are circularized by joining the 3'- and 5'-ends together.<sup>11</sup> At the molecular level, the circular RNA CiRS-7 contains many binding sites for the microRNA miR-7, and can function as a sponge of miR-7.<sup>12</sup> While most of the circular RNAs reported so far have been exonic circular RNAs, a class of intron-containing exonic circRNAs (ElciRNAs) are found predominantly in the nucleus,<sup>13</sup> where they promote transcription of their parental genes.<sup>14</sup> However, the functions of circular RNAs are largely unknown. We hypothesize that circ-Foxo3 plays physiological and pathological role at cellular and tissue levels. This study was designed to explore the potential effect of circ-Foxo3 on stress-induced senescence.

## Results

### Expression of circ-Foxo3 promoted senescence

We tested our hypothesis by generating a circ-Foxo3 expression construct, the sequence of which is identical to all variants of Foxo3. Total RNA was isolated from cardiac tissues from patients of different ages. Real-time polymerase chain reaction (PCR) analysis showed that heart tissues obtained from younger patients expressed lower levels of circ-Foxo3 than those from aging patients (Figure 1A). We also performed a similar experiment in murine hearts and found that the hearts of older mice expressed significantly higher levels of circ-Foxo3 than those from young mice (Figure 1B, left). By immunohistochemical staining, we found that the young tissues displayed undetectable staining of  $\beta$ -Gal, a well-accepted marker for senescence, whereas the old hearts showed extensive  $\beta$ -Gal staining (Figure 1B, right). We performed *in situ* hybridization for circ-Foxo3 expression and found that the old hearts expressed significantly higher levels of circ-Foxo3 than the young hearts (Figure 1C). We also found that both circ-Foxo3 and  $\beta$ -Gal were highly expressed in intestinal, lung, and dermal tissues in mice from the aged group, relative to the young group (Supplementary material online, Figure S1A). We explored the effects of circ-Foxo3 on senescence. The levels of circ-Foxo3 in a number of cell lines including mouse embryonic fibroblasts (MEFs), mouse cardiac

fibroblasts (MCFs), NIH3T3 fibroblasts, B16 cells, and primary cardiomyocytes were analysed. When the cells were treated with H<sub>2</sub>O<sub>2</sub>, significant levels of cellular senescence were detected (Figure 1D, Supplementary material online, Figure S1B). The treated cells were found to express significantly higher levels of circ-Foxo3 than the untreated cells (Figure 1E).

To corroborate these results, we designed an siRNA specifically targeting circ-Foxo3. We delivered the siRNA into MEFs and confirmed that transfection with this siRNA silenced circ-Foxo3 levels (Supplementary material online, Figure S1C). We also delivered an siRNA targeting the linear mRNA of Foxo3 into the cells. The cells transfected with circ-Foxo3 siRNA showed less  $\beta$ -gal staining than the cells transfected with Foxo3 siRNA or the control oligo (Figure 2A). Primary cardiomyocytes transfected with the siRNA also displayed lower levels of beta-Gal staining and circ-Foxo3 expression (Figure 2B, Supplementary material online, Figure S1D).

We developed methods to directly test the role of circ-Foxo3 in senescence. Mouse embryonic fibroblasts were transfected with circ-Foxo3 followed by Northern blotting. We detected strong up-regulation of circ-Foxo3 (Figure 2C). Three cell lines selected confirmed expression of circ-Foxo3 by RT-PCR and real-time PCR (Figure 2D). Circ-Foxo3- and mock-transfected MEFs were treated with H<sub>2</sub>O<sub>2</sub> followed by  $\beta$ -Gal staining. We found that all three circ-Foxo3-transfected cell lines underwent cellular senescence (Figure 2E).

### Effect of circ-Foxo3 on Doxorubicin-induced cardiomyopathy in mice

Since Dox is a chemotherapeutic drug that induces cellular stress and has been linked to cardiomyopathy of the treated individuals, we sought to determine whether circ-Foxo3 played a role in Dox-induced cardiomyopathy in mice. M-mode pictures of echocardiography was obtained, confirming the successful establishment of a mouse model of cardiomyopathy induced by Dox (Figure 3A). In the Dox-treated mice, both the left ventricular end diastolic diameter (LVEDD) and left ventricular end-systolic diameters (LVESD) were significantly increased in the Dox-treated mice compared with the control (Figure 3B). Consistent with these, the left ventricular ejection fraction, left ventricular fractional shortening, left ventricular systolic pressure (LVSP), and rate of rise of left ventricular pressure (dp/dt) were significantly decreased in the Dox-treated mice compared with the control (Figure 3C). When the circ-Foxo3 plasmid was delivered to the Dox-treated mice, we observed even higher levels of LVEDD and LVESD (Figure 3B), but lower levels of LVEF, LVFS, LVSP, and dp/dt (Figure 3C). When the siRNA-targeting endogenous circ-Foxo3 was delivered into the Dox-treated mice, the observed results were abrogated: significantly lower levels of LVEDD and LVESD (Figure 3B), but higher levels of LVEF, LVFS, LVSP, and dp/dt (Figure 3C).

Real-time PCR analysis of the cardiac tissues showed that Dox treatment increased circ-Foxo3 levels (Figure 3D, upper). Delivery of the circ-Foxo3 plasmid generated the highest expression levels of circ-Foxo3, whereas transfection of circ-Foxo3 siRNA decreased circ-Foxo3 levels (Figure 3D, upper). Circ-Foxo3 expression was found to be well correlated with the levels of tissue apoptosis, as

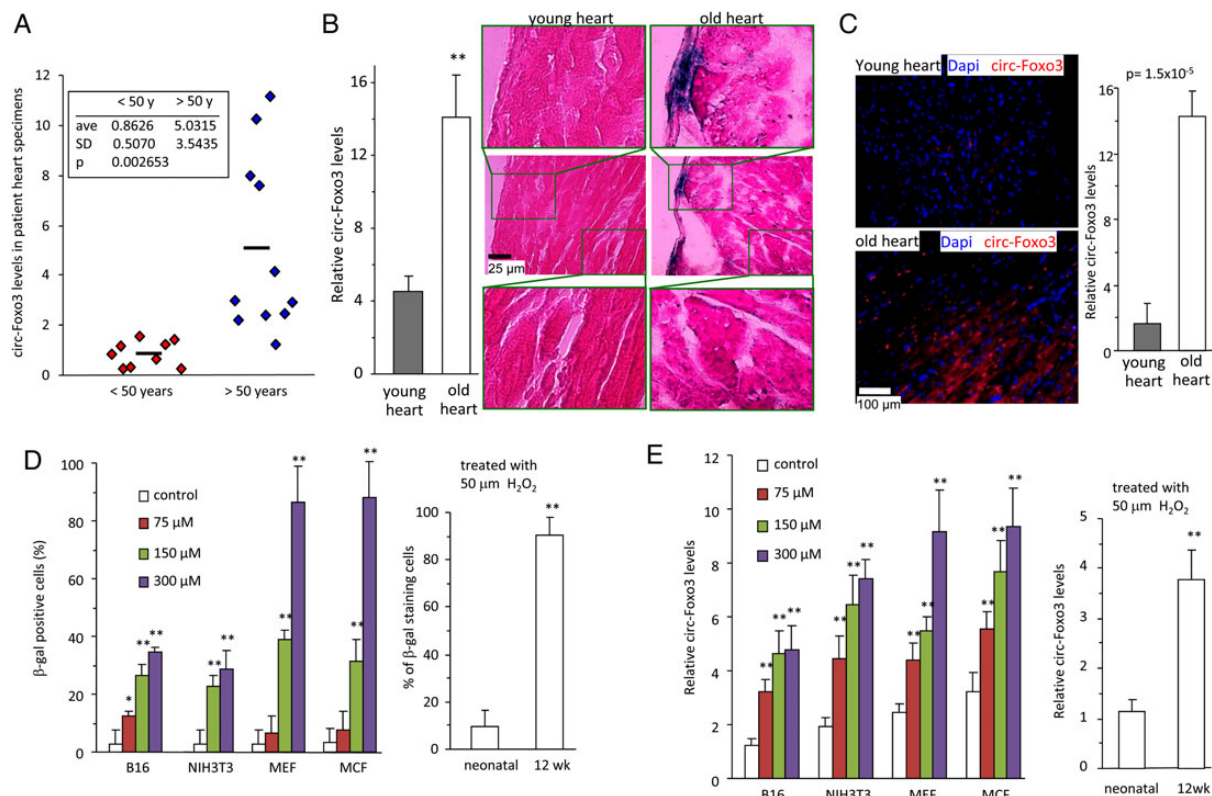


**Figure 1** Expression of circ-Foxo3 in young and old hearts. (A) Total RNAs were isolated from 20 specimens of patients (9 younger than 50 years and 11 older than 50 years) and subject to real-time polymerase chain reaction. The elder hearts expressed significantly higher levels of circ-Foxo3 than the younger hearts. (B) Left: Real-time polymerase chain reaction showed that the old hearts expressed significantly higher levels of circ-Foxo3 than the young heart. Right: The young tissues expressed undetectable staining of β-Gal, whereas the old hearts showed extensive β-Gal staining. (C) Left: The old tissues expressed higher levels of circ-Foxo3, but the young tissues showed very weak staining. Right: Statistical analysis showed a significant difference of 9-fold of β-Gal staining in the old heart compared with the young hearts. (D and E) Mouse cell lines including mouse embryonic fibroblast, mouse cardiac fibroblast, NIH3T3, B16, and primary cardiomyocytes isolated from neonatal and 12-week hearts were treated with H<sub>2</sub>O<sub>2</sub>. Significantly higher levels of senescent cells were detected (D). RNAs were subject to real-time polymerase chain reaction to measure circ-Foxo3 levels (E). In all experiments provided, asterisks indicate significant differences, where \**P* < 0.05 and \*\**P* < 0.01. Error bars means standard deviation.

measured by TUNEL staining (Figure 3D, lower, Supplementary material online, Figure S1E).

HE staining revealed a dilated LV chamber in Dox-treated mice (Figure 3E). Ectopic expression of circ-Foxo3 generated further dilated LV chambers, while silencing endogenous circ-Foxo3 decreased the size of LV chamber (Figure 3E). Cardiac fibrosis was examined by collagen expression using Sirlus-Red staining. Doxorubicin treatment increased collagen staining, which was amplified by ectopic circ-Foxo3 expression, while silencing circ-Foxo3 expression decreased collagen staining (Supplementary material online, Figure S1F). The levels of β-Gal staining increased in the Dox-treated heart. The levels were even higher in the circ-Foxo3-transfected heart, while silencing circ-Foxo3 decreased β-Gal levels (Figure 3F). This was correlated by circ-Foxo3 expression in the heart tissues displayed by *in situ* hybridization (Supplementary material online, Figure S2A). These results demonstrated that increased circ-Foxo3 levels promoted tissue deterioration, whereas silencing endogenous circ-Foxo3 appeared to slow down this process. Immunostaining with α-SMA, an ideal marker

for cardiomyocytes in response to stresses or injury during tissue remodelling,<sup>15</sup> confirmed circ-Foxo3 hybridization occurred inside the cells (Supplementary material online, Figure S2B).

## Interaction of circ-Foxo3 with Id1, E2F1, HIF1α, and FAK

We tested for potential interactions of circ-Foxo3 with the senescence-associated proteins ID1 and E2F1. Since stress has important effects on senescence, the anti-stress proteins FAK and HIF1α were examined. The precipitated mixture was subject to real-time PCR using primers specific for the linear Foxo3 mRNA and circ-Foxo3. The experiment showed that circ-Foxo3 was pulled down by antibodies against ID1, E2F1, FAK, and HIF1α, but the linear Foxo3 mRNA was not (Figure 4A, upper). We confirmed these results by preparing RNAs from the vector- and circ-Foxo3-transfected MEFs. Antibodies against these proteins pulled down significantly higher levels of circ-Foxo3 from the

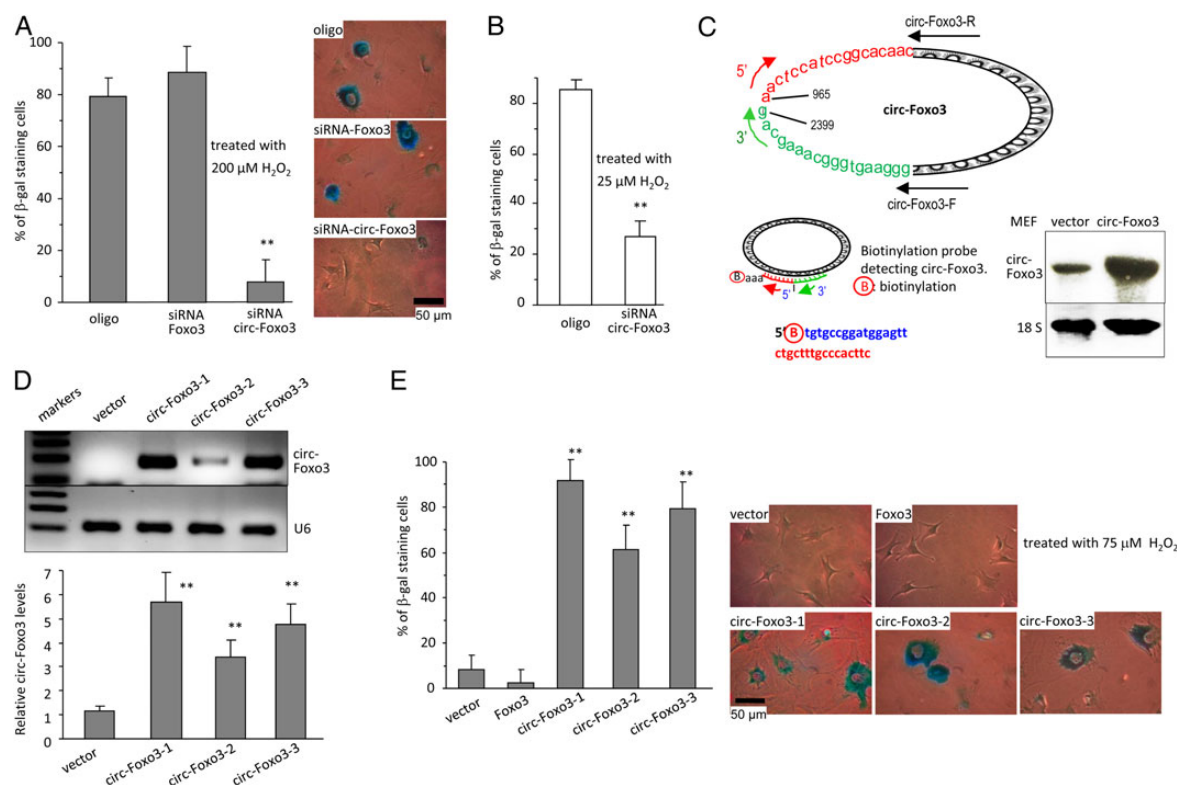


**Figure 2** Expression of circ-Foxo3 promoted cellular senescence. (A) Left: After being treated with 200  $\mu$ M H<sub>2</sub>O<sub>2</sub> for 2 h, and then cultured in basal medium for 48 h, mouse embryonic fibroblasts transfected with Foxo3 siRNA, circ-Foxo3 siRNA, or a control oligo were subject to  $\beta$ -gal staining. The circ-Foxo3 siRNA-transfected mouse embryonic fibroblasts showed significantly decreased  $\beta$ -gal staining compared with those transfected with Foxo3 siRNA or the control oligo. \*\* $P < 0.01$ ; error bars, SD ( $n = 6$ ). Right: typical photos of  $\beta$ -gal staining. (B) Primary cardiomyocytes isolated from neonatal and 12-week heart tissues were treated with 25  $\mu$ M H<sub>2</sub>O<sub>2</sub> followed by  $\beta$ -Gal staining. Cells isolated from the mature tissues displayed significantly more  $\beta$ -Gal-positive cells relative to the cells isolated from mature tissues. \*\* $P < 0.01$ ; error bars, SD ( $n = 6$ ). (C) Left: Structures and probe sequence of circ-Foxo3. Right: Northern blotting showed increased circ-Foxo3 expression. (D) Upper: RT-polymerase chain reaction showed that three cell lines stably transfected with circ-Foxo3 expressed high levels of circ-Foxo3. Lower, real-time polymerase chain reaction showed that circ-Foxo3-transfected mouse embryonic fibroblasts expressed significantly higher levels of circ-Foxo3. \*\* $P < 0.01$ ; error bars, SD ( $n = 4$ ). (E) Left: treated with 75  $\mu$ M H<sub>2</sub>O<sub>2</sub> for 2 h, and then cultured in basal medium for 48 h, mouse embryonic fibroblasts transfected with circ-Foxo3 showed increased  $\beta$ -gal staining compared with cells transfected with the linear Foxo3 or the untransfected control. \*\* $P < 0.01$ ,  $n = 6$ . Right: typical photos of  $\beta$ -gal staining.

circ-Foxo3-transfected cells than those from vector-transfected cells (Figure 4A, lower).

To corroborate the interaction of circ-Foxo3 with Id1, E2F1, HIF1 $\alpha$ , and FAK, we used an siRNA approach to knock-down circ-Foxo3 in primary cardiomyocytes. Silencing endogenous circ-Foxo3 significantly decreased the levels of circ-Foxo3 pulled down by these proteins (Figure 4B).

We further tested the interactions between circ-Foxo3 and the proteins. Lysates from circ-Foxo3- or vector-transfected MEFs were incubated with a biotinylated probe designed to specifically detect circ-Foxo3. The mixture was subject to real-time PCR and the experiments showed that circ-Foxo3-transfected MEFs expressed high levels of circ-Foxo3 (Figure 4C, upper). The mixture was subject to a pull-down assay by incubation with streptavidin beads, followed by real-time PCR. We found that increased levels of circ-Foxo3 were pulled down by the probe compared with the control (Figure 4C, lower).

We then tested whether the probe was able to pull-down these proteins by adding it to the lysates prepared from MEFs transfected with circ-Foxo3. The mixtures were subject to Western blot probed with antibodies against these proteins to confirm that transfection with circ-Foxo3 did not affect expression of these proteins (Supplementary material online, Figure S3A). The mixtures were incubated with streptavidin beads, followed by western blotting. It was found that circ-Foxo3 could pull down Id1, E2F1, HIF1 $\alpha$ , and FAK from cells transfected with circ-Foxo3 (Figure 4D).

Lysates prepared from MEFs and primary cardiomyocytes transfected with circ-Foxo3 siRNA or an oligo were mixed with the biotinylated probes. Real-time PCR confirmed that transfection with circ-Foxo3 siRNA decreased circ-Foxo3 levels (Supplementary material online, Figure S3B). The pulled down RNAs were subject to real-time PCR. Significantly lower levels of circ-Foxo3 were pulled down by the probe compared with the control oligo (Figure 4E).



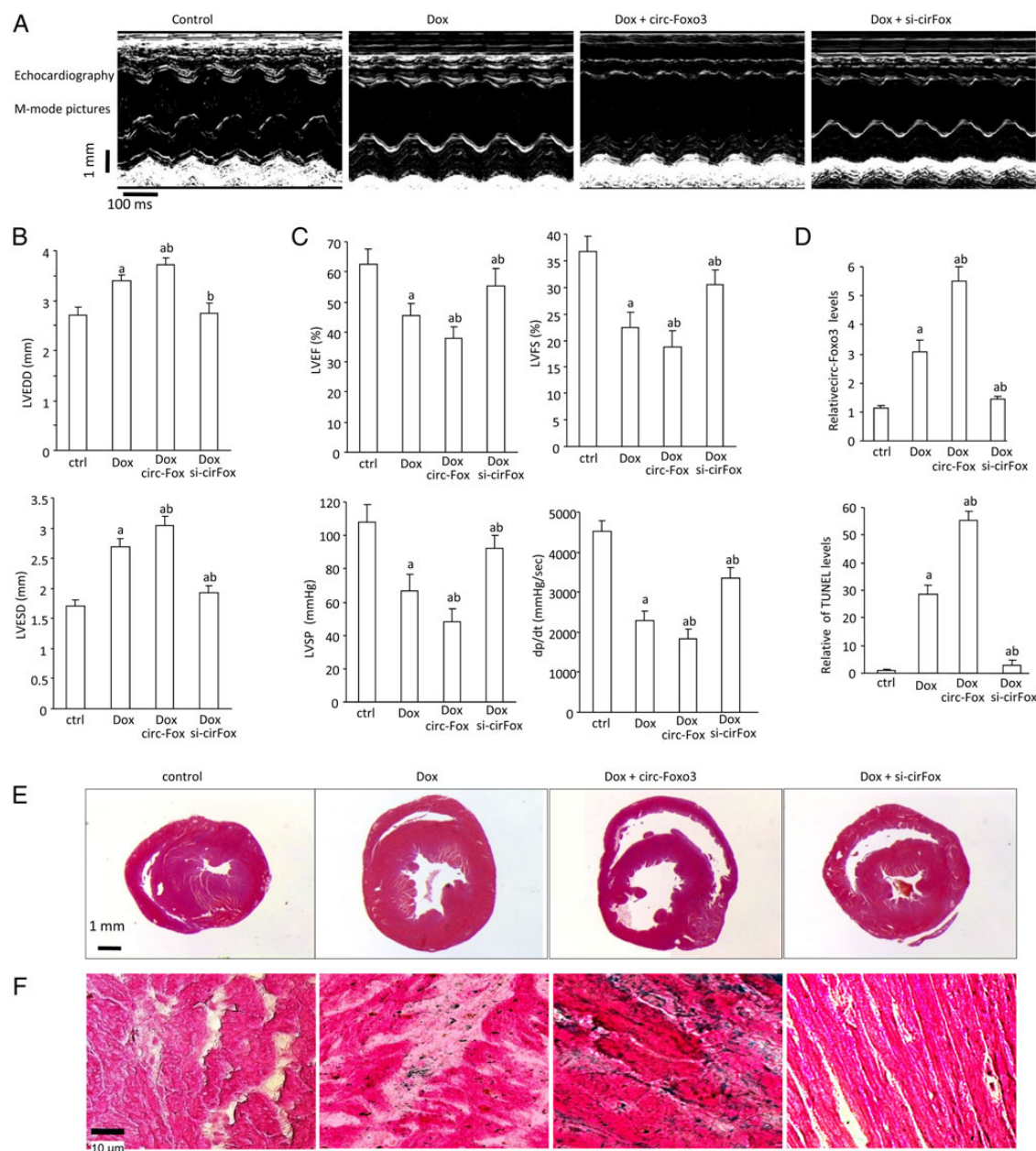


**Figure 3** Silencing circ-Foxo3 attenuated Doxorubicin-induced cardiomyopathy in mice. (A) Representative echocardiography photographs showing heart function in different groups. (B) Doxorubicin treatment increased mouse left ventricular end diastolic diameter (upper) and left ventricular end-systolic diameters (lower). Ectopic expression of circ-Foxo3 enhanced Doxorubicin-induced increase of left ventricular end diastolic diameter and left ventricular end-systolic diameters, while silencing circ-Foxo3 repressed Doxorubicin-induced increase of left ventricular end diastolic diameter and left ventricular end-systolic diameters (a,  $P < 0.01$  vs. control; b,  $P < 0.01$  vs. Doxorubicin; error bars, SD,  $n = 10$  mice). (C) Doxorubicin treatment reduced mouse LVEF, LVFS, LVSP, and dp/dt. Expression of circ-Foxo3 enhanced Doxorubicin-induced reduction of these parameters, while silencing circ-Foxo3 showed opposite effects (a,  $P < 0.01$  vs. control; b,  $P < 0.01$  vs. Doxorubicin; error bars, SD,  $n = 10$  mice). (D) Doxorubicin treatment increased circ-Foxo3 levels (upper), shown by real-time polymerase chain reaction, and apoptosis (lower), shown by TUNEL staining in mouse heart tissues. Ectopic expression of circ-Foxo3 enhanced Doxorubicin-induced expression of circ-Foxo3 and apoptosis, while silencing circ-Foxo3 decreased circ-Foxo3 expression and apoptosis (a,  $P < 0.01$  vs. control; b,  $P < 0.01$  vs. Doxorubicin; error bars, SD,  $n = 5$  mice). (E) Three weeks after Doxorubicin injection, heart sections were subject to H&E staining. Shown are representative photos. (F) Typical  $\beta$ -gal staining of heart tissues showing that Doxorubicin treatment induced mouse heart senescence, which was enhanced by overexpression of circ-Foxo3 and repressed by circ-Foxo3 silencing.

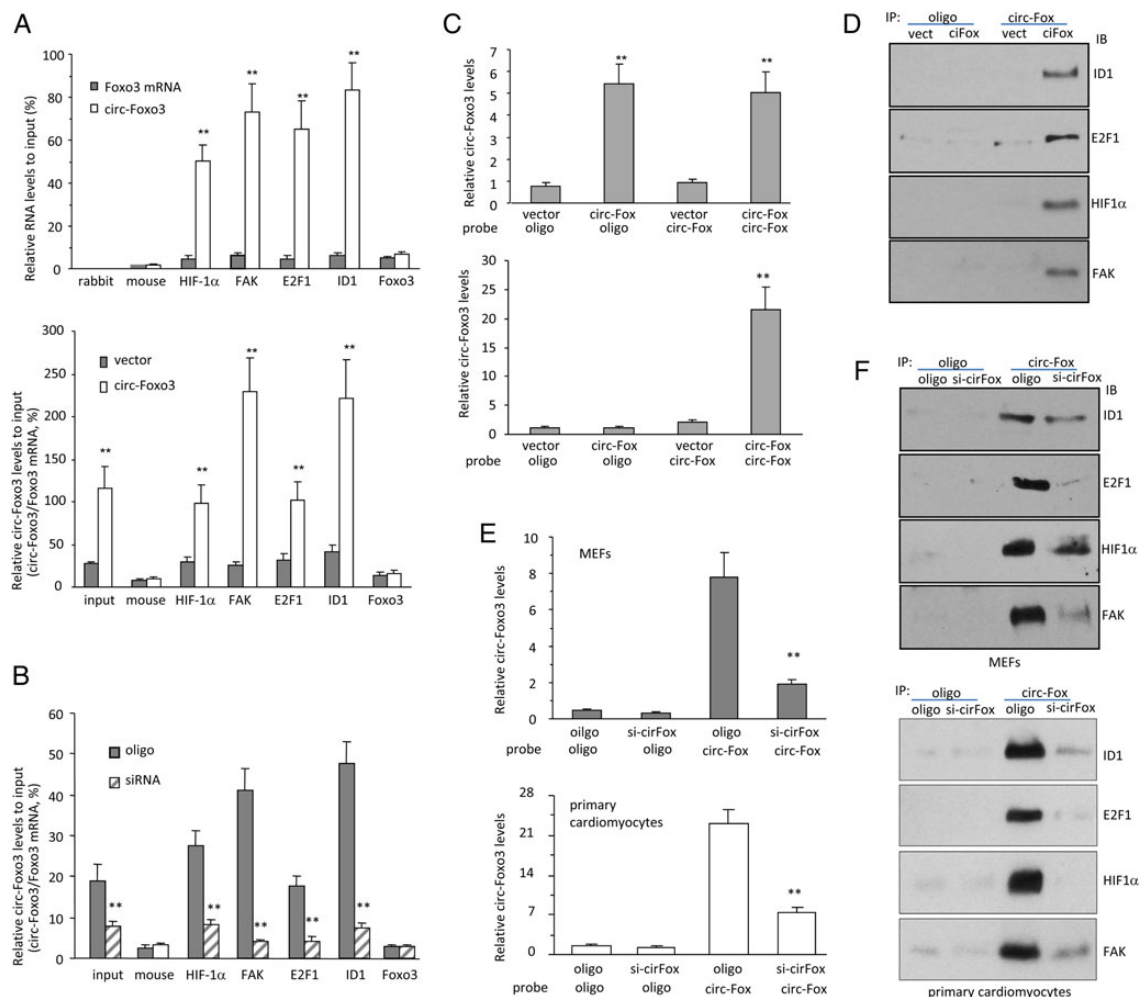


**Figure 4** Circ-Foxo3 interacted with ID1, E2F1, HIF1α, and FAK. (A) Upper: Cell lysis prepared from mouse embryonic fibroblasts were subject to immuno-precipitation with antibodies against rabbit IgG, mouse IgG, ID1, E2F1, HIF1α, FAK, and Foxo3, followed by real-time polymerase chain reaction. Antibodies against these proteins pulled down circ-Foxo3, but not Foxo3. Lower: Cell lysates were subject to immuno-precipitation followed by real-time polymerase chain reaction. Antibodies against these proteins pulled down more circ-Foxo3 from the circ-Foxo3-transfected cells.  $**P < 0.01$ , error bars, SD,  $n = 4$ . (B) Primary cardiomyocytes were transfected with circ-Foxo3 siRNA followed by immuno-precipitation assay. Antibodies against the indicated proteins pulled down less circ-Foxo3 from the siRNA-transfected cells.  $**P < 0.01$ , error bars, SD,  $n = 4$ . (C) Upper: The lysates were mixed with biotinylated probes against ectopic expressed circ-Foxo3 or a control oligo, followed by real-time polymerase chain reaction. Transfection with circ-Foxo3 expressed higher levels of circ-Foxo3 than the control. Lower: The mixtures were incubated with streptavidin beads followed by real-time polymerase chain reaction. The probe pulled down expressed circ-Foxo3.  $**P < 0.01$ , error bars, SD,  $n = 4$ . (D) The lysates were mixed with the biotinylated probes and incubated with streptavidin beads followed western blotting. The probe pulled down Id1, E2F1, HIF1α, and FAK but not in the other controls. (E) Upper: Cell lysates prepared from mouse embryonic fibroblasts transfected with siRNA-targeting circ-Foxo3 or a control oligo were mixed with the biotinylated probes and incubated with streptavidin beads followed by real-time polymerase chain reaction. The circ-Foxo3 probe pulled down lower levels of circ-Foxo3 in the siRNA-transfected cells than in the control.  $**P < 0.01$ , error bars, SD,  $n = 4$ . Lower: Primary cardiomyocytes were subject to similar assays and similar results were obtained. (F) Upper: The lysates were mixed with the biotinylated probes and incubated with streptavidin beads followed western blotting. The probe pulled down decreased levels of Id1, E2F1, HIF1α, and FAK in the circ-Foxo3-transfected cells than those transfected with a control oligo. Lower: Primary cardiomyocytes were subject to similar assays.

The probe was added to the lysates. The mixtures were subject to western blot to confirm that transfection with circ-Foxo3 siRNA did not affect expression of Id1, E2F1, HIF1α, or FAK (Supplementary material online, Figure S3C). In pull-down assays, the probe pulled down decreased levels of these proteins from circ-Foxo3-transfected cells (Figure 4F).

### Effect of circ-Foxo3 on subcellular translocation of ID1, E2F1, HIF1α, and FAK

Levels of circ-Foxo3 were analysed in RNA isolated from cytoplasmic and nuclear fractions. Similar to the linear Foxo3 and GAPDH mRNAs, circ-Foxo3 was mainly detected in cytoplasm (Figure 5A).

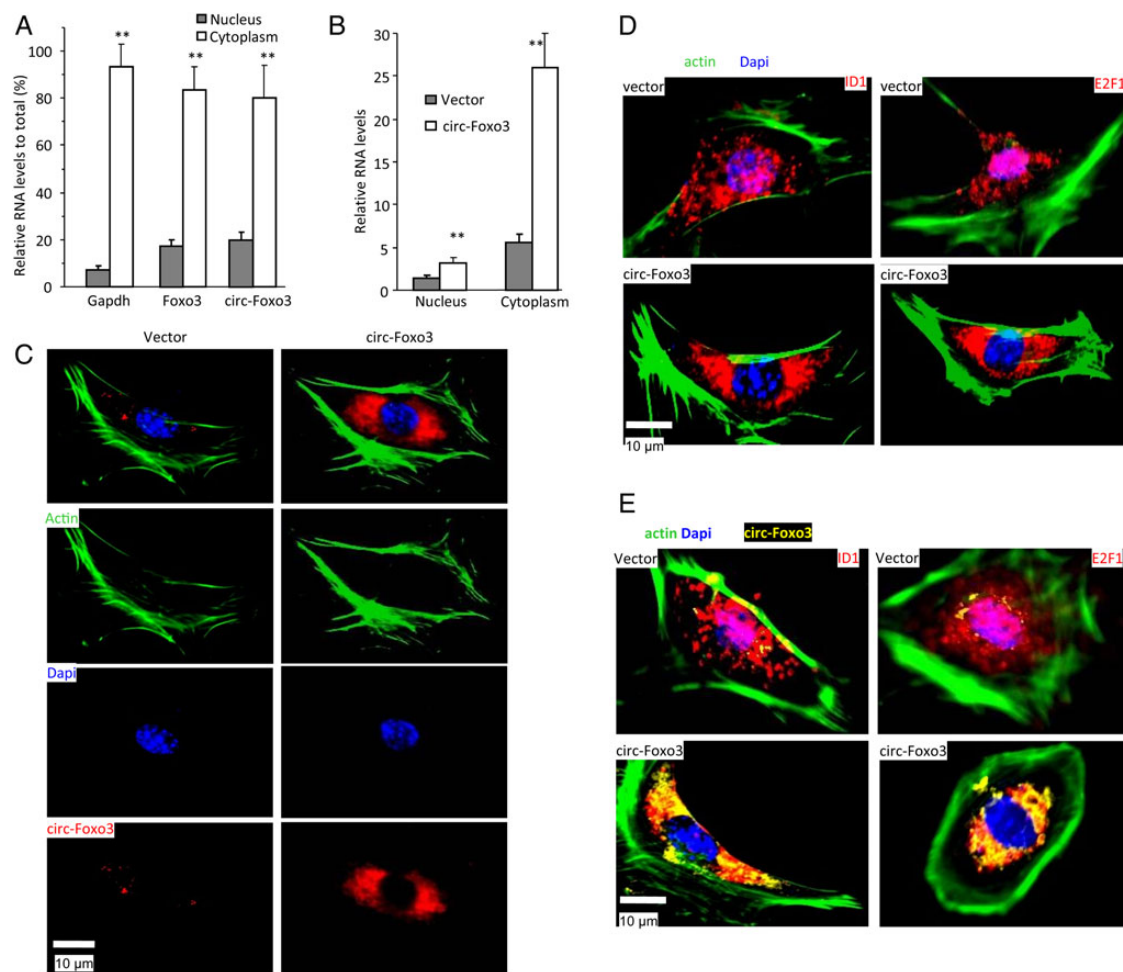


**Figure 5** Expression of circ-Foxo3 affected Id1, E2F1, HIF1 $\alpha$ , and FAK subcellular translocation. (A) RNAs prepared from the nucleus and cytoplasm of mouse embryonic fibroblasts were subject to real-time polymerase chain reaction. circ-Foxo3 was mainly expressed in the cytoplasm as GAPDH and Foxo3 did.  $**P < 0.01$ , error bars, SD,  $n = 4$ . (B) RNAs prepared from the nucleus and cytoplasm of mouse embryonic fibroblasts transfected with circ-Foxo3 or mock control were subject to real-time polymerase chain reaction. The ectopically expressed circ-Foxo3 was mainly detected in the cytoplasm.  $**P < 0.01$ , error bars, SD,  $n = 4$ . (C) circ-Foxo3- or mock-transfected mouse embryonic fibroblasts were stained with phalloidin, DAPI, and circ-Foxo3. Most of circ-Foxo3 was detected in cytoplasm. (D) Circ-Foxo3 transfection decreased nuclear translocation of ID1 and E2F1. (E) Circ-Foxo3 was found co-localized with ID1 and E2F1 in cytoplasm.

In addition, the circ-Foxo3-transfected cells expressed significantly higher levels of circ-Foxo3 in the cytoplasm and nucleus than the controls did (Figure 5B). The circ-Foxo3- and vector-transfected MEFs were also subject to *in situ* hybridization. The ectopically expressed circ-Foxo3 was mainly distributed in the cytoplasm (Figure 5C).

We validated the effects of circ-Foxo3 on the nuclear translocation of ID1, E2F1, and HIF1 $\alpha$ . In the vector-transfected cells, both ID1 and E2F1 were detected in the cytoplasm and nucleus, whereas ectopic expression of circ-Foxo3 facilitated localization of most ID1 and E2F1 to the cytoplasm (Figure 5D, complete panel of sections in Supplementary material online, Figure S4A). This was consistent with the distribution of circ-Foxo3 in the cytoplasm (Figure 5E, Supplementary material online, Figure S4B).

We performed similar immunostaining and *in situ* hybridization of the heart sections. We detected increased levels of circ-Foxo3 in the Dox-treated tissues and the circ-Foxo3-transfected tissues,

but decreased levels in the circ-Foxo3 silencing group (Supplementary material online, Figure S5A and B). The increased circ-Foxo3 facilitated co-localization of E2F1 (Supplementary material online, Figure S5A) and ID1 (Supplementary material online, Figure S5B) in the cytoplasm instead of the nuclei. Similarly, HIF1 $\alpha$  distribution was also co-localized with circ-Foxo3 in the cytoplasm instead of the nuclei (Supplementary material online, Figure S6A), whereas FAK distribution was co-localized in the cytoplasm outside the mitochondria (Supplementary material online, Figure S6B), in a similar fashion to their staining in cell culture (Supplementary material online, Figure S4A and B).

We tested whether cellular stress affected expression and translocation of Id1, E2F1, HIF1 $\alpha$ , and FAK. The circ-Foxo3- or mock-transfected MEFs were treated with H<sub>2</sub>O<sub>2</sub> followed by western blotting. Among HIF1 $\alpha$ , FAK, E2F1, and ID1, only HIF1 $\alpha$  was up-regulated in both circ-Foxo3- and mock-transfected cells (Figure 6A).

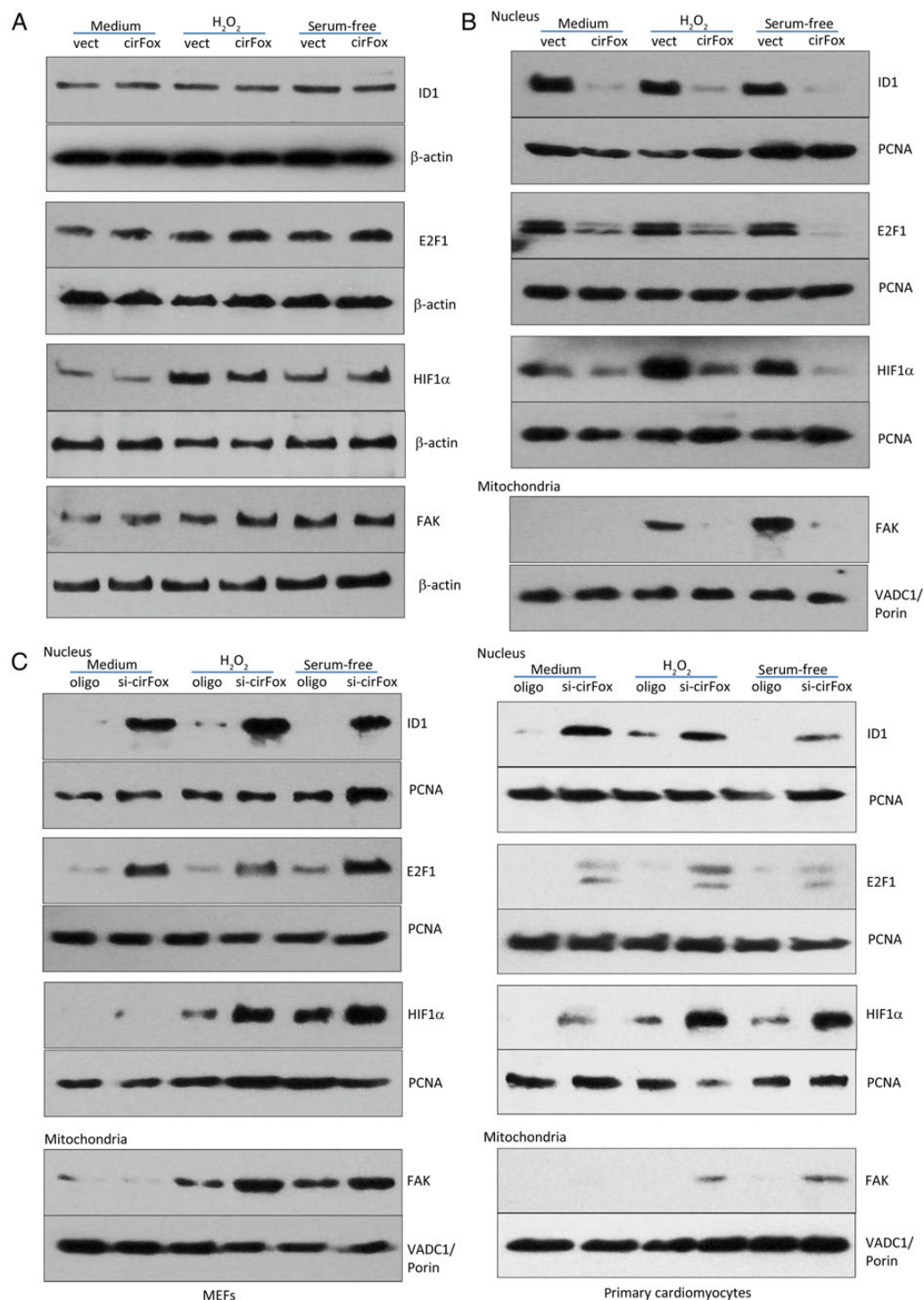


**Figure 6** Translocation of Id1, E2F1, HIF1 $\alpha$ , and FAK in response to stress (A) circ-Foxo3- and vector-transfected mouse embryonic fibroblasts were cultured in basal medium or serum-free medium for 48 h, or treated with 75  $\mu$ M H<sub>2</sub>O<sub>2</sub> for 2 h, followed by western blotting. Expression of HIF1 $\alpha$  was up-regulated in both circ-Foxo3- and vector-transfected cells cultured in serum-free medium or treated with H<sub>2</sub>O<sub>2</sub>. (B) Upper: nuclear fractions were prepared for western blotting. circ-Foxo3 transfection decreased levels of Id1, E2F1, and HIF1 $\alpha$ . All membranes were reprobated with PCNA antibody to confirm equal loading. Lower, in mitochondria, stress only increased levels of FAK in the vector-transfected cells but not in the circ-Foxo3-transfected cells. The membranes were reprobated with VDAC1/Porin antibody to confirm equal loading. (C) The effect of circ-Foxo3 on translocation of ID1, E2F1, HIF1 $\alpha$ , and FAK was tested by transfection of circ-Foxo3 siRNA in mouse embryonic fibroblasts (left) and primary cardiomyocytes (right) after stress. In the nuclear fractions, siRNA transfection increased levels of ID1, E2F1, and HIF1 $\alpha$ . Similarly, level of FAK increased in mitochondria after stress and transfection with circ-Foxo3 siRNA further increased FAK level.



In nuclear fractions, while we detected approximately equal levels of PCNA, we found that the levels of HIF1 $\alpha$ , E2F1, and ID1 decreased greatly in the circ-Foxo3-transfected cells compared with the control (Figure 6B, upper). Treatment with H<sub>2</sub>O<sub>2</sub> or cultured in serum-free medium did not produce an additional effect on ID1 and E2F1 expression, but appeared to generate a greater difference for HIF1 $\alpha$  expression between circ-Foxo3- and mock-transfected cells. In mitochondria, while no difference of VDAC1/Porin was found, stress increased FAK levels in the vector-transfected cells but not in the circ-Foxo3-transfected cells (Figure 6B, lower).

To corroborate these results, we delivered circ-Foxo3 siRNA into MEFs and primary cardiomyocytes, which did not affect expression of the proteins (Supplementary material online, Figure S3D). Knocking down endogenous circ-Foxo3 enhanced expression of ID1 and E2F1 in the nucleus (Figure 6C). It also enhanced HIF1 $\alpha$  expression in the nucleus after H<sub>2</sub>O<sub>2</sub> treatment. In mitochondria, knocking down endogenous circ-Foxo3 enhanced FAK expression in stressed cells.

We confirmed the distributions of HIF1 $\alpha$  and FAK by *in situ* hybridization. In normal culture medium, HIF1 $\alpha$  levels were relatively low in the nucleus, but treatment with H<sub>2</sub>O<sub>2</sub> greatly increased HIF1 $\alpha$  levels in the nucleus (Figure 7A, complete panel in

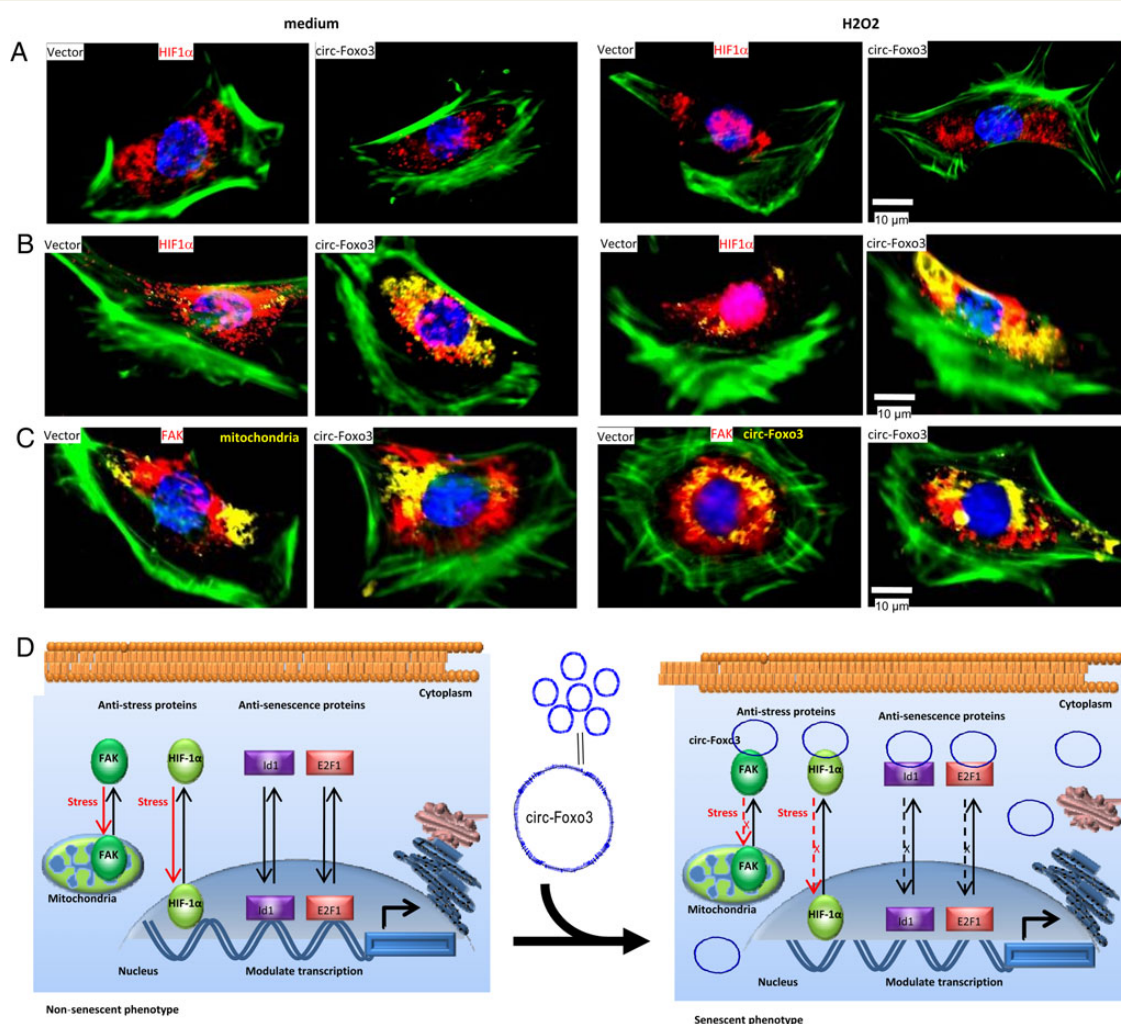


**Figure 7** Co-localization of HIF1 $\alpha$  and FAK with circ-Foxo3 in response to stress (A) circ-Foxo3- and vector-transfected mouse embryonic fibroblasts were cultured in basal medium or treated with 75  $\mu$ M H<sub>2</sub>O<sub>2</sub> for 2 h, followed by immunocytochemistry and confocal microscopic examination. Transfection with circ-Foxo3 retained HIF1 $\alpha$  in cytoplasm even after H<sub>2</sub>O<sub>2</sub> treatment. (B) HIF1 $\alpha$  was co-localized with circ-Foxo3 in cytoplasm. (C) Left: Distinct distribution of FAK and mitochondria was observed when the cells were cultured in normal medium. Right: Treatment with H<sub>2</sub>O<sub>2</sub> facilitated co-localization of FAK and circ-Foxo3 in the vector-transfected cells, but expression of circ-Foxo3 retained the distinct distribution of FAK and circ-Foxo3. (D) Summary of the results. Most of the circ-Foxo3 was expressed in cytoplasm, where it could bind senescence-related proteins ID1 and E2F1, and stress-related proteins HIF1 $\alpha$  and FAK. Expression of circ-Foxo3 decreased ID1 and E2F1 in the nucleus. circ-Foxo3 also decreased HIF1 $\alpha$  in nucleus and FAK in mitochondria after the cells were treated with H<sub>2</sub>O<sub>2</sub> or cultured in serum-free medium.

Supplementary material online, Figure S7A). This was consistent with the distribution of circ-Foxo3: treatment with H<sub>2</sub>O<sub>2</sub> did not affect distribution of circ-Foxo3, resulting in detection of both circ-Foxo3 and HIF1 $\alpha$  in the cytoplasm (Figure 7B, complete panel in Supplementary material online, Figure S7B). Treatment with H<sub>2</sub>O<sub>2</sub> had little effect on the distribution of the expressed circ-Foxo3, in a similar pattern as the untreated cells (Figure 7C, complete panel in Supplementary material online, Figure S8A).

## Discussion

In this study, we found that circ-Foxo3 was highly expressed in the tissues of aged mice and patients. The levels of circ-Foxo3 in mouse hearts were correlated with markers of senescence. To examine the role of circ-Foxo3 in cardiac function, we adopted a mouse model of Dox-induced cardiomyopathy. We found that the ectopic expression of circ-Foxo3 aggravated Dox-induced cardiomyopathy, but silencing endogenous circ-Foxo3 reduced the Dox-induced effects and exerted a cardio-protective effect. We found that ectopic expression of circ-Foxo3 induced cellular senescence of MEFs, where it interacted with the anti-senescence proteins ID1 and E2F1, and anti-stress proteins FAK and HIF1 $\alpha$ . These interactions prevented nuclear translocation of these transcription factors, causing cytoplasmic retention and reduced function. Since ID1, E2F1, and HIF1 $\alpha$  are transcription factors, it is essential for them to enter into the nucleus to exert their functional roles. The interactions of circ-Foxo3 and these transcription factors appear to arrest their functions.

ID1 is known to play roles in cell growth, differentiation, and premature replicative senescence.<sup>16</sup> Forced overexpression of ID1 delays replicative senescence.<sup>17</sup> Our results are consistent with these reports in that, when ID1 protein was bound to cytoplasmic circ-Foxo3, ID1 could no longer function as a transcription factor, and cellular senescence was promoted. Knockout of the transcription factor E2F1 induces bone-marrow-derived macrophage senescence.<sup>18</sup> Partial repression of E2F1 also increases cell senescence. Ectopic expression of miR-205 induces senescent phenotypes in melanoma by elevating expression of senescent markers.<sup>19</sup> E2F1 overexpression in miR-205-expressing cells was found to partially reverse the senescent phenotype. In our study, we showed that the expression of E2F1 was not affected by ectopic expression of circ-Foxo3, but the translocation of E2F1 was largely blocked by circ-Foxo3 expression. It is hypothesized that the function of E2F1 as a transcription factor was inhibited, thereby promoting cellular senescence.

Regulation of HIF1 $\alpha$  expression by either hypoxia or genetic alternations has been implicated in cancer biology and senescence. Negative regulation of HIF1 $\alpha$  induces cancer cell senescence.<sup>20</sup> We found that treatment with H<sub>2</sub>O<sub>2</sub> induced HIF1 $\alpha$  expression, but in the circ-Foxo3-transfected cells, HIF1 $\alpha$  was detected mainly in cytoplasm. This was in contrast to HIF1 $\alpha$  produced from vector-transfected cells, which was found to localize predominantly to the nucleus. Our results support previous reports that reducing HIF1 $\alpha$  function promotes cellular senescence.

FAK is a focal adhesion-associated protein kinase involved in cellular adhesion and spreading. FAK mediates intracellular signal pathways and promote the turn-over of cell contacts and cell migration,

thus modulating cellular senescence. Down-regulation of uPAR resulted in decreased activity in FAK/PI3K/Akt pathway and increased senescence-associated nuclear morphology and up-regulation of  $\beta$ -galactosidase activity.<sup>21</sup> In our study, we found that inducing oxidative stress increased FAK expression. However, in the circ-Foxo3-transfected cells, FAK was arrested in the cytoplasm, which appeared to contribute to the increased cellular senescence.

Previous results indicated that increased cellular senescence may slow-down tumor cell proliferation, migration, invasion, and metastasis. Senescence may function beneficially in the inhibition of tumor progression and extend the lifespan of cancer patients. However, in healthy individuals, senescence likely causes deterioration and reduction in normal functioning. This may increase the likelihood of pathological processes, in shortening lifespan. Thus, senescence heavily affects physiological and pathological conditions. Understanding the mechanisms contributing to cellular senescence is a subject of current scientific focus.

In summary, our study demonstrated that ectopic expressed circ-Foxo3 was mainly detected in cytoplasm, where it could bind to senescence-related proteins ID1 and E2F1, and stress-related proteins HIF1 $\alpha$  and FAK. Both HIF1 $\alpha$  and FAK also exerted negative effects on senescence. Increased amounts of circ-Foxo3 in the cytoplasm resulted in arresting ID1, E2F1, HIF1 $\alpha$ , and FAK in cytoplasm, decreasing levels of these proteins in the nucleus. The anti-senescent function of these proteins was thereby blocked. As a result, ectopic expression of circ-Foxo3 was found to promote cellular senescence (Figure 7D), while silencing circ-Foxo3 decreased cell senescence and apoptosis. Our *in vivo* delivery of siRNA-targeting endogenous circ-Foxo3 abrogating the effect of Dox provides a potential therapeutic approach for myocardial protection.

## Methods

Senescence-associated  $\beta$ -galactosidase staining was performed as described.<sup>9</sup> Protein assays on western blot and immunohistochemistry were performed as described.<sup>22,23</sup> Real-time PCR was conducted as described.<sup>24–26</sup> The detailed methods are provided in Supplementary methods online.

## Statistical analysis

All experiments were performed in triplicate or as indicated and numerical data were subject to independent sample *t*-test. The levels of significance were set at \**P* < 0.05 and \*\**P* < 0.01.

## Supplementary material

Supplementary material is available at *European Heart Journal* online.

## Authors' contributions

W.W.D. performed statistical analysis. B.B.Y. handled funding and supervision. W.W.D., Y.C., Z.Y., X.L. acquired the data. W.W.D., W.Y., B.B.Y. conceived and designed the research. W.W.Y., W.W.D., B.B.Y. drafted the manuscript. W.W.Y., W.W.D., B.B.Y. made critical revision of the manuscript for key intellectual content.

## Funding

This work was supported by a Discovery Grant from the Natural Sciences and Engineering Research Council of Canada (NSERC; 227937-2012) to B.B.Y., who is the recipient of a Career Investigator Award (CI 7418) from the Heart and Stroke Foundation of Ontario. W.W.D. is supported by a Postdoctoral Fellowship from the Breast Cancer Foundation of Ontario. Z.Y. is supported by a Scholarship from China Scholarship Council.

**Conflict of interest:** none declared.

## References

- Ohtani N, Zebedee Z, Huot TJ, Stinson JA, Sugimoto M, Ohashi Y, Sharrocks AD, Peters G, Hara E. Opposing effects of ETS and ID proteins on p16INK4a expression during cellular senescence. *Nature* 2001;**409**:1067–1070.
- Rodier F, Campisi J. Four faces of cellular senescence. *J Cell Biol* 2011;**192**:547–556.
- Wang Z, Wei D, Xiao H. Methods of cellular senescence induction using oxidative stress. *Methods Mol Biol* 2013;**1048**:135–144.
- Stein GH, Drullinger LF, Robetorye RS, Pereira-Smith OM, Smith JR. Senescent cells fail to express cdc2, cycA, and cycB in response to mitogen stimulation. *Proc Natl Acad Sci USA* 1991;**88**:11012–11016.
- Harley CB, Futcher AB, Greider CV. Telomeres shorten during ageing of human fibroblasts. *Nature* 1990;**345**:458–460.
- Kurz DJ, Decary S, Hong Y, Erusalimsky JD. Senescence-associated (beta)-galactosidase reflects an increase in lysosomal mass during replicative ageing of human endothelial cells. *J Cell Sci* 2000;**113**(Pt 20):3613–3622.
- Du WW, Li X, Li T, Li H, Khorshidi A, Liu F, Yang BB. The microRNA miR-17-3p inhibits mouse cardiac fibroblast senescence by targeting Par4. *J Cell Sci* 2015;**128**:293–304.
- Shan SW, Lee DY, Deng Z, Shatseva T, Jeyapalan Z, Du WW, Zhang Y, Xuan JW, Yee SP, Siragam V, Yang BB. MicroRNA MiR-17 retards tissue growth and represses fibronectin expression. *Nat Cell Biol* 2009;**11**:1031–1038.
- Du WW, Yang W, Fang L, Xuan J, Li H, Khorshidi A, Gupta S, Li X, Yang BB. miR-17 extends mouse lifespan by inhibiting senescence signaling mediated by MKP7. *Cell Death Dis* 2014;**5**:e1355.
- Minotti G, Ronchi R, Salvatorelli E, Menna P, Cairo G. Doxorubicin irreversibly inactivates iron regulatory proteins 1 and 2 in cardiomyocytes: evidence for distinct metabolic pathways and implications for iron-mediated cardiotoxicity of antitumor therapy. *Cancer Res* 2001;**61**:8422–8428.
- Jeck WR, Sharpless NE. Detecting and characterizing circular RNAs. *Nat Biotechnol* 2014;**32**:453–461.
- Hansen TB, Jensen TI, Clausen BH, Bramsen JB, Finsen B, Damgaard CK, Kjems J. Natural RNA circles function as efficient microRNA sponges. *Nature* 2013;**495**:384–388.
- Li X, Wu Q, Xie Y, Ding Y, Du WW, Sdiri M, Yang BB. Ergosterol purified from medicinal mushroom *Amauroderma rude* inhibits cancer growth in vitro and in vivo by up-regulating multiple tumor suppressors. *Oncotarget* 2015; **6**:17832–17846.
- Li Z, Huang C, Bao C, Chen L, Lin M, Wang X, Zhong G, Yu B, Hu W, Dai L, Zhu P, Chang Z, Wu Q, Zhao Y, Jia Y, Xu P, Liu H, Shan G. Exon-intron circular RNAs regulate transcription in the nucleus. *Nat Struct Mol Biol* 2015;**22**:256–264.
- Kern S, Feng HZ, Wei H, Cala S, Jin JP. Up-regulation of alpha-smooth muscle actin in cardiomyocytes from non-hypertrophic and non-failing transgenic mouse hearts expressing N-terminal truncated cardiac troponin I. *FEBS Open Bio* 2013;**4**:11–17.
- Perk J, Iavarone A, Benezra R. Id family of helix-loop-helix proteins in cancer. *Nat Rev Cancer* 2005;**5**:603–614.
- Nickoloff BJ, Chaturvedi V, Bacon P, Qin JZ, Denning MF, Diaz MO. Id-1 delays senescence but does not immortalize keratinocytes. *J Biol Chem* 2000;**275**:27501–27504.
- Iglesias-Ara A, Zenarruzabeitia O, Fernandez-Rueda J, Sanchez-Tillo E, Field SJ, Celada A, Zubiaga AM. Accelerated DNA replication in E2F1- and E2F2-deficient macrophages leads to induction of the DNA damage response and p21(CIP1)-dependent senescence. *Oncogene* 2010;**29**:5579–5590.
- Dar AA, Majid S, de Semir D, Nosrati M, Bezrookove V, Kashani-Sabet M. miRNA-205 suppresses melanoma cell proliferation and induces senescence via regulation of E2F1 protein. *J Biol Chem* 2011;**286**:16606–16614.
- Kato H, Inoue T, Asanoma K, Nishimura C, Matsuda T, Wake N. Induction of human endometrial cancer cell senescence through modulation of HIF-1alpha activity by EGLN1. *Int J Cancer* 2006;**118**:1144–1153.
- Nowicki TS, Zhao H, Darzynkiewicz Z, Moscatello A, Shin E, Schantz S, Tiwari RK, Geliebter J. Downregulation of uPAR inhibits migration, invasion, proliferation, FAK/PI3K/Akt signaling and induces senescence in papillary thyroid carcinoma cells. *Cell Cycle* 2011;**10**:100–107.
- Du WW, Liu F, Shan SW, Ma XC, Gupta S, Jin T, Spaner D, Krylov SN, Zhang Y, Ling W, Yang BB. Inhibition of dexamethasone-induced fatty liver development by reducing miR-17-5p levels. *Mol Ther* 2015;**23**:1222–1233.
- Yang BL, Cao L, Kiani C, Lee V, Zhang Y, Adams ME, Yang BB. Tandem repeats are involved in G1 domain inhibition of versican expression and secretion and the G3 domain enhances glycosaminoglycan modification and product secretion via the complement-binding protein-like motif. *J Biol Chem* 2000;**275**:21255–21261.
- Rutnam ZJ, Du WW, Yang W, Yang X, Yang BB. The pseudogene TUSC2P promotes TUSC2 function by binding multiple microRNAs. *Nat Commun* 2014;**5**:2914.
- Shan SW, Fang L, Shatseva T, Rutnam ZJ, Yang X, Du W, Lu WY, Xuan JW, Deng Z, Yang BB. Mature miR-17-5p and passenger miR-17-3p induce hepatocellular carcinoma by targeting PTEN, GalNT7 and vimentin in different signal pathways. *J Cell Sci* 2013;**126**(Pt 6):1517–1530.
- Yang W, Du WW, Li X, Yee AJ, Yang BB. Foxo3 activity promoted by non-coding effects of circular RNA and Foxo3 pseudogene in the inhibition of tumor growth and angiogenesis. *Oncogene* 2015 Dec 14. doi: 10.1038/onc.2015.460. [Epub ahead of print].